Supporting Information

Revealing the bonding environment of Zn in ALD Zn(O,S) Buffer Layers through X-ray Absorption Spectroscopy

*Anup Dadlani,[1] Shinjita Acharya,[2] Orlando Trejo,[2] Dennis Nordlund,[3] Mirco Peron,[4] Javad Razavi,[4] Filippo Berto,[4] Fritz B. Prinz,[2,5] and Jan Torgersen[2,4]**

[1] Department of Chemistry, Stanford University, Stanford, CA 94305

[2] Department of Mechanical Engineering, Stanford University, Stanford, CA 94305, USA

[3] Stanford Synchrotron Radiation Lightsource, SLAC National Accelerator Laboratory, Menlo Park, USA

[4] Department of Mechanical and Industrial Engineering, NTNU Trondheim, Trondheim, Norway

[5] Department of Materials Science and Engineering, Stanford University, Stanford, CA 94305, USA

* Corresponding Author

Email: jan.torgersen@ntnu.no

Experimental Methods

X-ray photoluminescence (XPS) was done using PHI Versa Probe Scanning XPS Microprobe which uses Al (Kα) radiation of 1486 eV in a vacuum environment of $5*10^{-7}$ Torr. Data not shown here as data was published in prior work.[1]

XRD on the samples was performed in a PANalytical X'Pert PRO X-ray diffraction system. The grazing incidence angle omega was set to 0.5° and Cu Kα radiation with a wavelength of 1.540598 Å was used. Relevant data from previous work is rehashed below.

ALD of Zn(O,S) films

The substrates were loaded into a customized flow-type ALD system. The substrate temperature was maintained at 160 °C. Diethylzinc (DEZ), distilled H_2O, and a gas mixture of 3.5% H_2S in N_2 were used as precursors to deposit Zn(O,S). The pulse time for all precursors was 0.1 s, their residence time in the reaction chamber was 2 s to ensure complete saturation of the available surface sites. After each precursor pulse, 45 s were allotted for byproduct evacuation. Conventionally, ZnO and ZnS films were deposited in a laminar fashion pulsing DEZ into the reaction chamber before its oxidation with either H_2O or H_2S. Both ALD films are well characterized in literature.[2,3] Zn(O,S) composition was adjusted by employing different ratios of ZnS cycles within the total number of ALD cycles (ZnO+ZnS) as previously reported.[4] In addition to the nanolaminate deposition technique, we propose an alternative diffusion based deposition method (Diffd) employing a set number of H_2S cycles after each ZnO deposition. To differentiate between Zn(O,S) compositions deposited with either method, we refer to the oxidant pulse ratio ($H_2S/(H_2O+H_2S)$) for comparison. Zn(O,S) samples of three different S compositions were fabricated and are described by the H_2S oxidant pulse ratios 33%, 20% and 10%, respectively.

Two types of substrates were used: Si substrates and TiO_2 nanoparticles (NPs). The Si substrates were 500 μm thick p-doped Si <100> (WRS materials). TiO_2 NPs were prepared on quartz substrates as previously reported.[5] On either substrate, five pulses of H_2O were employed prior to ALD of ZnO and Zn(O,S) to ensure proper nucleation (and the growth of a native SiO_2 on Si). For ZnS deposition, we pulsed five H_2S pulses onto the substrates prior to the deposition.

The sample labels follow the form lettersnumber_cycles, where letters indicate substrate (S for SiO_2, T for TiO_2 NPs), number indicates the H_2S to total number of oxidant pulses, and cycles tells the total number of cycles of ALD deposition. In each case, Zn(O,S) layers were deposited using 10, 20, and 33% of $H_2S/(H_2S+H_2O)$ ALD oxidant pulses

X-ray photoluminescence (XPS) and Atomic Force Microscopy (AFM) was done on these Zn(O,S) films in our prior works[1,6] to check stoichiometry and to check for consistency with previous reports.[4,7]

XANES for Zinc K-edge measurements

At BL 11-2, the samples were positioned at 45° from both the incident x-ray beam and the detector. The energy X-ray slits were approximately set to 1 mm x 10 mm. A 30-element Ge solid state Detector Array detector was used to gather the total fluorescence yield (TFY) data.

XANES for Zinc LIII, LII-edge measurements

Total electron yield (TEY) spectra were gathered at BL 10-1. To measure the sample drain current for the TEY data, all samples were loaded on the sample stick with carbon tape and were electrically grounded with carbon paste.

Zinc K and L edge spectra

All spectra were background subtracted and atomically normalized in the energy region from 9690 to 9700 eV.

The Zn LIII, LII-edge XANES total electron yield (TEY) spectra of thick samples (300 cycles) deposited on SiO_2 are shown in Fig. S2a. The same spectra is replicated in the main text except for the fact that it only shows the LIII-edge. The LIII-edge was the main focus of our analysis as the L-II edge is both weaker in intensity and also does not even start at the same energy for all the samples. In Fig. S2b, the derivative spectra is a longer range than what is shown in the main text. The more important region of the derivative spectra is the beginning peak and hence a shorter range is plotted in the main text. The sharpness and intensity of the first peak is an indicator of ionicity in the metal edge, where with increasing sulfur content the ionicity increases. While there are a few differences later on in the spectra, the spectra also suffer from worse S/N ratio there.

In Fig. S3a, the derivative of the thick (darker curves) and thin (lighter curves) are plotted together. It is observed that the thicker samples all have an earlier onset for the first peak compared to their thinner counterparts. This likely suggests that the band gaps of the thicker films is probably smaller than the thinner films. It can also be noted that fewer peaks appear for the thinner samples, which is expected given the lack of long range order having been developed. The derivative of thick and thin films at the Zn LIII-edge is plotted in Fig. S3b. The 10% samples have much overlap in the spectrum and indeed their XANES spectra look similar. The thin 20% and 33% samples have a sharper first peak which may stem from the presence of zinc sulfate.

The spectra shown in Fig. S4 are similar to Fig. 4 in the main text. The difference is that the LII edge is also provided here and the derivative spectra shows a wider range.

In Fig. S5, as in our previous work on thin films (O K-edge), a comparison of the films deposited by the conventional nanolaminate method and our Diff'd method is shown. It can be seen that the spectra are quite similar to each other even though the ALD pulse sequence was drastically different. This is a strong indication that the films should behave similarly as one would expect the geometric and electronic structure to be quite similar. It illustrates that more investigation is necessary into the growth of ALD thin films, particularly in sulfide ternary films.

In Fig. S6a and Fig. S6b more films of different thickness fabricated using the Diff'd method are shown at the LIII-edge and LIII, LII-edges respectively. Sulfur rich films seem to have an extra degree of tunability, which is by varying the thickness of these films their electronic and geometric structure can be significantly altered. The sulfur films here are intermediate in thickness (150 cycles) which shows differences both from the thin (20 cycles) and thick (300 cycles) samples.

GIXRD measurement

The crystallographic data for the samples was obtained by GIXRD. The data is shown in our previous work. Below is the curve for ZnO, which is necessary in explaining the large A peak present in the Zn K edge for our ZnO sample that is otherwise not seen in literature. In literature the A peak is visible but is not as prominent as seen in our XANES spectrum. It can be seen in Fig. S1 that the ZnO grown by ALD has a strongly preferred orientation favoring the (200) plane. Due to this preferred orientation, when the XANES is performed with the configuration

used, we probe a substantial sigma character of the Zn 4s orbitals that contributes to the A peak and hence the A peak we observe is much greater that what is reported in literature.

Simulations

We demonstrate the nature of bonding through multiple-scattering simulations of ZnO and ZnS clusters. Theoretical XANES spectra are simulated using the FEFF9 code[8],[9] based on Green's function multiple-scattering theory where the parameters SCF (specifies the radius of the cluster for full multiple scattering during the self-consistency loop) and FMS (computes full multiple scattering within a sphere of radius **r** centered on the absorbing atom) were changed. We first obtained spectral agreement between simulated and experimental wurtzite ZnO and spahlerite ZnS at the Zn K edge.

LDOS

The LDOS was calculated for all the simulated XANES spectra that has been shown, using FEFF9. The partial density of states (pDOS) were then properly aligned to the Fermi level by shifting the total density of states (tDOS) so that the onset of the band gap was at 0 eV. Next the experimental curves were aligned by shifting it so that the highest intensity was in line with the highest intensity of the pDOS of the absorbing anion. Fig. 2b, d shows the pDOS curves placed underneath the pertinent experimental curves in the main text.

(a)

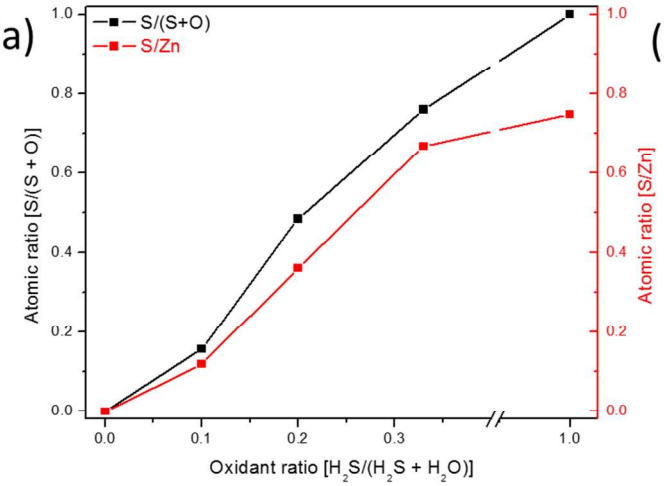

(b)

Sample	Density (g/cm^3)	Thickness (nm)
ZnO_300	4.9	58.38
10%_300	4.3	58.42
20%_160	3.73	27.87
33%_300	3.6	50.87
ZnS_300	3.55	33.86

Figure S1: ALD Zn(O,S) recipes and corresponding compositions. (a) Composition and (b) thicknesses measured by means of X-ray photoluminescence (XPS) and X-ray reflectivity (XRR), respectively. Modified from ref 1.

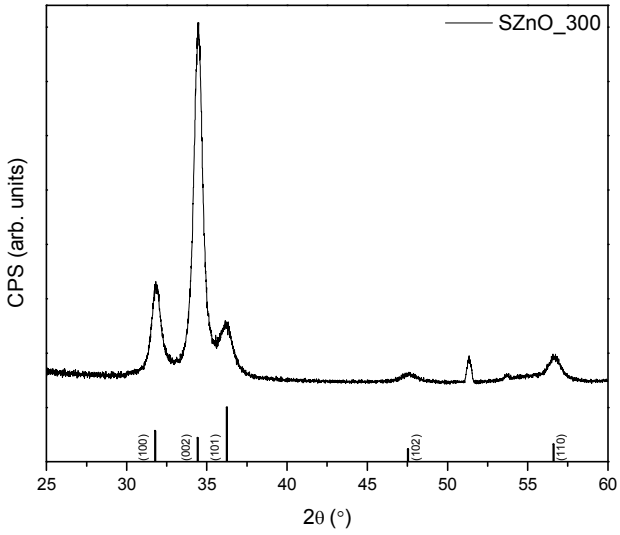

Figure S2: Grazing incidence diffractogram of ZnO film (160 °C, Si <100>, 300 cycles).

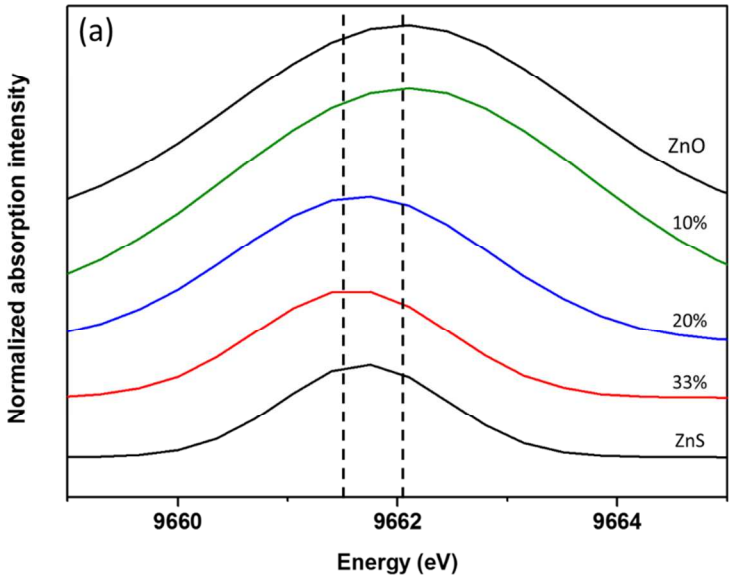

(b)	Centre (eV)	FWHM (eV)	R^2
ZnO	9662,063	3,1343	0,99981
10_300	9662,096	3,2589	0,99975
20_300	9661,678	2,35766	0,99884
33_300	9661,588	1,75313	0,99996
ZnS	9661,698	1,5035	0,99995

Figure S3: Fitted peaks at the onset of the Zn-K edge spectra for Zn(O,S) films of different S concentrations. The peaks get sharper and higher in intensity with the integration of S. Furthermore, the onset shifts to lower energy (a) peaks at different S concentrations (b) centre, FWHM, and R^2 value of peaks.

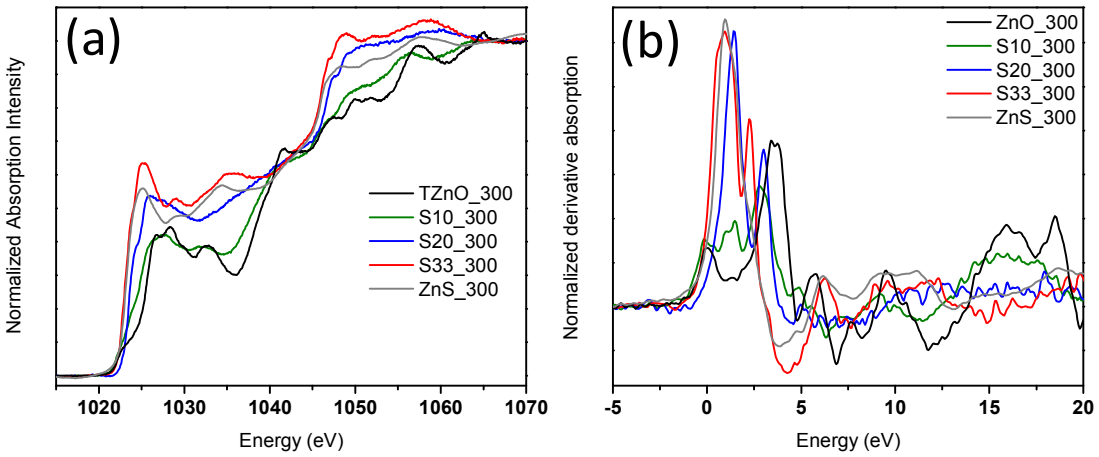

Figure S4: (a) The Zn LIII (1025 eV), LII-edge (1045 eV) XANES TEY spectra of Zn(O,S) thick films of varying S composition deposited on a silicon wafer. **(b)** The derivative spectra for the films show sharper and larger first peaks just like in the K-edge which indicates a system that is getting more ionic with the incorporation of a greater sulfur content.

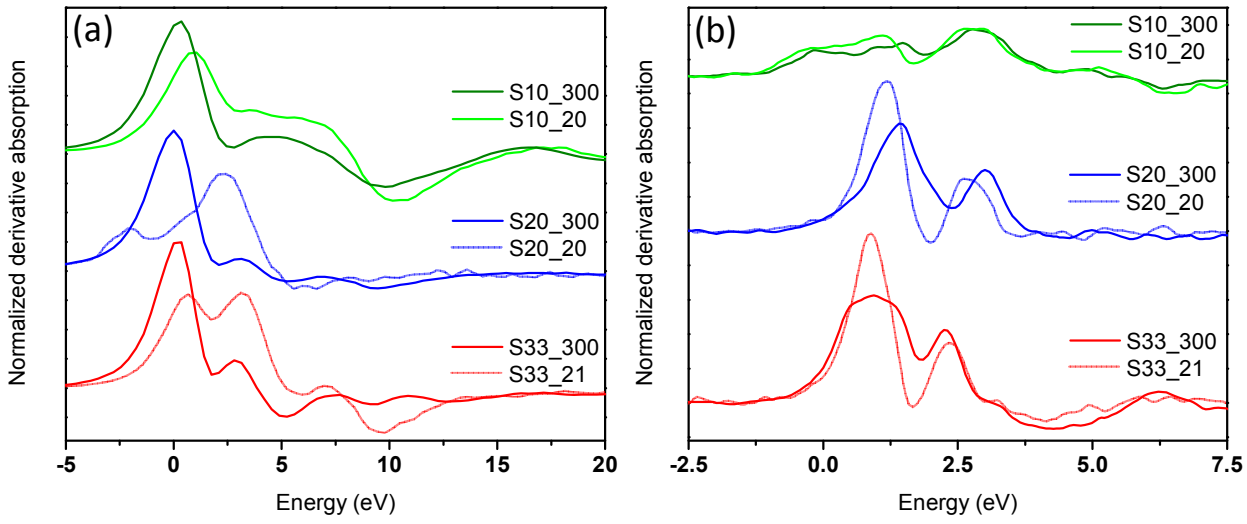

Figure S5: (a) The derivative of thick and thin films at the Zn K-edge. Onset of the main peak for the thin films is at higher energies which could be indicative of higher band gaps. **(b)** The derivative of the thick and thin samples at the Zn LIII-edge. The 10% samples overlap significantly, while the 20% and 33% have sharper first peaks, possibly due to formation of zinc sulfate.

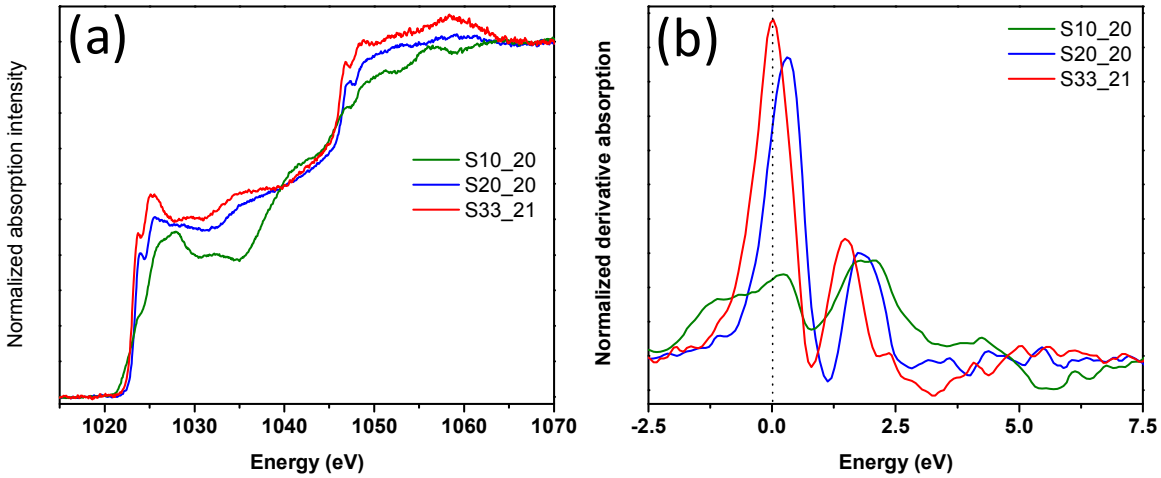

Figure S6: (a) The Zn LIII,LII-edge XANES TEY spectra of Zn(O,S) thin films of varying S composition deposited on silicon wafer. The 10% sample looks much like the thicker counterpart except for a stronger appearing shoulder. Both the 20% and 33% samples are also similar to their thicker films except the shoulder now appears as a peak. We speculate it might be the case that some zinc sulfate might be present at the interface as we oberved in our previous work. **(b)** the normalized derivative spectra for samples in (a). As seen in the main text, the higher sulfur content sample has a stronger and sharper first peak in the derivative which means it is the most ionic. This is then followed by the 20% and the 10% respectively.

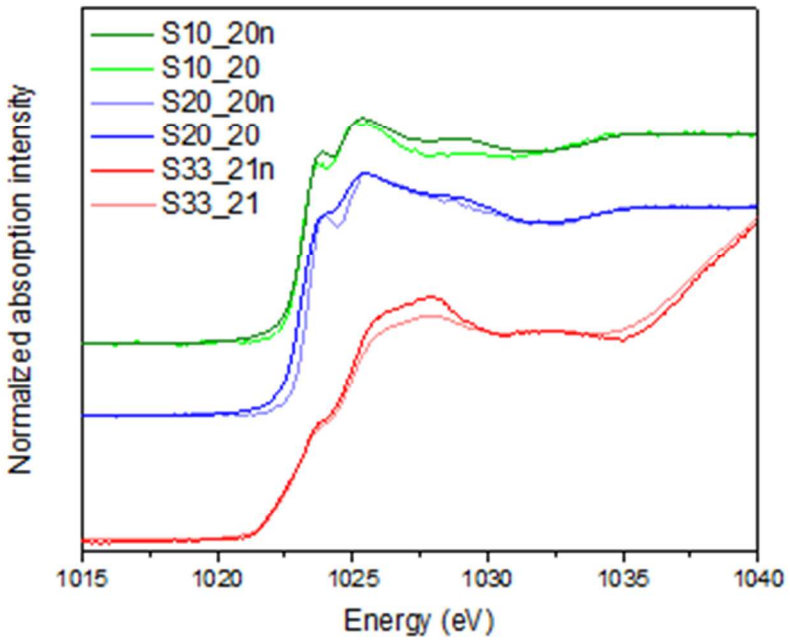

Figure S7: The Zn LIII-edge XANES TEY spectra of Zn(O,S) thin films of varying S composition deposited using the conventional laminar method and our diffusion facilitated deposition method (Diffd), demarcated by "n" on a silicon wafer. As in our previous manuscript, the samples fabricated by either method have similar looking spectra, with very minor

differences, suggesting that the films have similar electronic and geometric stuctures and hence should behave similarly.

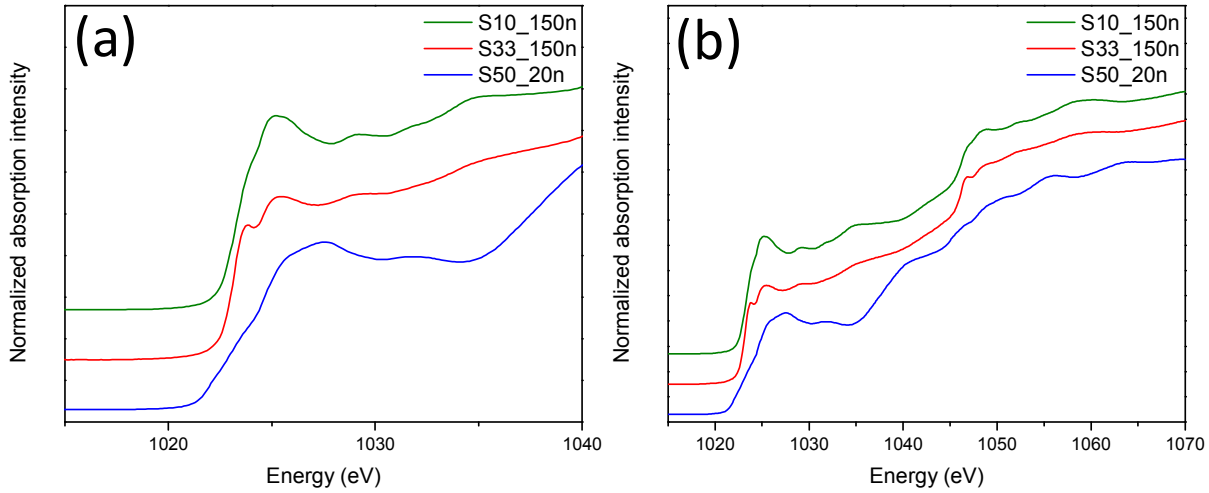

Figure S8: (a) The Zn LIII-edge XANES TEY spectra of Zn(O,S) films of varying S composition deposited using our diffusion facilitated deposition method (Diffd), demarcated by "n" on a silicon wafer. The 10% sample which is half as thick looks very much like thick samples grown the conventional way (Figure 3). The 33% sample is also only half as thick as the thick sample, looks quite a bit different from the thick sample. It appears the S rich films have a wide range of tunability (oxidant ratio and thickness). The 50% thin sample looks most similar to 33% thin film grown by either deposition strategy but the shoulder and main peaks are less pronounced. **(b)** Zn LIII, LII-edge XANES TEY spectra (same as in (a) but showing the Zn LII-edge also).

References

(1) Dadlani, A. L.; Trejo, O.; Acharya, S.; Torgersen, J.; Petousis, I.; Nordlund, D.; Sarangi, R.; Schindler, P.; Prinz, F. B. Exploring Local Electronic Structure and Geometric Arrangement of ALD Zn(O,S) Buffer Layers Using X-Ray Absorption Spectroscopy. *J. Mater. Chem. C* **2015**, *3* (47), 12192–12198.

(2) Boichot, R.; Tian, L.; Richard, M.-I.; Crisci, A.; Chaker, A.; Cantelli, V.; Coindeau, S.; Lay, S.; Ouled, T.; Guichet, C.; Chu, M. H.; Aubert, N.; Ciatto, G.; Blanquet, E.; Thomas, O.; Deschanvres, J.-L.; Fong, D. D.; Renevier, H. Evolution of Crystal Structure During the Initial Stages of ZnO Atomic Layer Deposition. *Chem. Mater.* **2016**, *28* (2), 592–600.

(3) Stuyven, G.; De Visschere, P.; Hikavyy, A.; Neyts, K. Atomic Layer Deposition of ZnS Thin Films Based on Diethyl Zinc and Hydrogen Sulfide. *J. Cryst. Growth* **2002**, *234* (4), 690–698.

(4) Platzer-Björkman, C.; Törndahl, T.; Abou-Ras, D.; Malmström, J.; Kessler, J.; Stolt, L. Zn(O,S) Buffer Layers by Atomic Layer Deposition in Cu(In,Ga)Se[sub 2] Based Thin Film Solar Cells: Band Alignment and Sulfur Gradient. *J. Appl. Phys.* **2006**, *100* (4), 44506.

(5) Trejo, O.; Roelofs, K. E.; Xu, S.; Logar, M.; Sarangi, R.; Nordlund, D.; Dadlani, A. L.;

Kravec, R.; Dasgupta, N. P.; Bent, S. F. Quantifying Geometric Strain at the PbS QD-TiO2 Anode Interface and Its Effect on Electronic Structures. *Nano Lett.* **2015**, *15* (12), 7829–7836.

(6) Dadlani, A. L.; Acharya, S.; Trejo, O.; Prinz, F. B.; Torgersen, J. ALD Zn (O, S) Thin Films' Interfacial Chemical and Structural Configuration Probed by XAS. *ACS Appl. Mater. Interfaces* **2016**, *8* (23), 14323−14327.

(7) Bakke, J. R.; Tanskanen, J. T.; Hägglund, C.; Pakkanen, T. A.; Bent, S. F. Growth Characteristics, Material Properties, and Optical Properties of Zinc Oxysulfide Films Deposited by Atomic Layer Deposition. *J. Vac. Sci. Technol. A* **2012**, *30* (1), 01A135.

(8) Rehr, J. J.; Kas, J. J.; Vila, F. D.; Prange, M. P.; Jorissen, K. Parameter-Free Calculations of X-Ray Spectra with FEFF9. *Phys. Chem. Chem. Phys.* **2010**, *12* (21), 5503–5513.

(9) Rehr, J. J.; Kas, J. J.; Prange, M. P.; Sorini, A. P.; Takimoto, Y.; Vila, F. Ab Initio Theory and Calculations of X-Ray Spectra. *C. R. Phys.* **2009**, *10* (6), 548–559.